Supplemental Information for

Mechanism for enhanced eolian dust flux recorded in North Pacific Ocean sediments since 4.0 Ma: aridity or humidity at dust source areas in the Asian interior?

Qiang Zhang[1, 2], Qingsong Liu[3, *], Andrew P. Roberts[4], Juan C. Larrasoaña[5, 6], Xuefa Shi[7], and Chunsheng Jin[1]

[1] *State Key Laboratory of Lithospheric Evolution, Institute of Geology and Geophysics, Chinese Academy of Sciences, 100029, Beijing, China.*

[2] *College of Earth and Planetary Sciences, University of Chinese Academy of Sciences, 100049, Beijing, China.*

[3] *Centre for Marine Magnetism (CM[2]), Department of Ocean Science and Engineering, Southern University of Science and Technology, 518055, Shenzhen, China.*

[4] *Research School of Earth Sciences, Australian National University, Canberra, ACT 2601, Australia.*

[5] *Instituto Geológico y Minero de España, Unidad del IGME en Zaragoza, C/ Manuel Lasala 44 9ºB, 50006 Zaragoza, Spain.*

[6] *Institute of Earth Sciences Jaume Almera ICTJA-CSIC, C/ Solé i Sabarís s/n, 08028 Barcelona, Spain.*

[7] *Key Laboratory of Marine Sedimentology and Environmental Geology, First Institute of Oceanography, Ministry of Natural Resources (MNR), 266061, Qingdao, China.*

*Corresponding author: Qingsong Liu (qsliu@sustech.edu.cn, Tel: +86 0755-88018789)

Contents of this file

5) Part 5: La-Th-Sc diagram for ODP Hole 885A

6) Part 6: Land-ocean comparison between the Chinese Loess Plateau (CLP) and North Pacific Ocean (NPO)

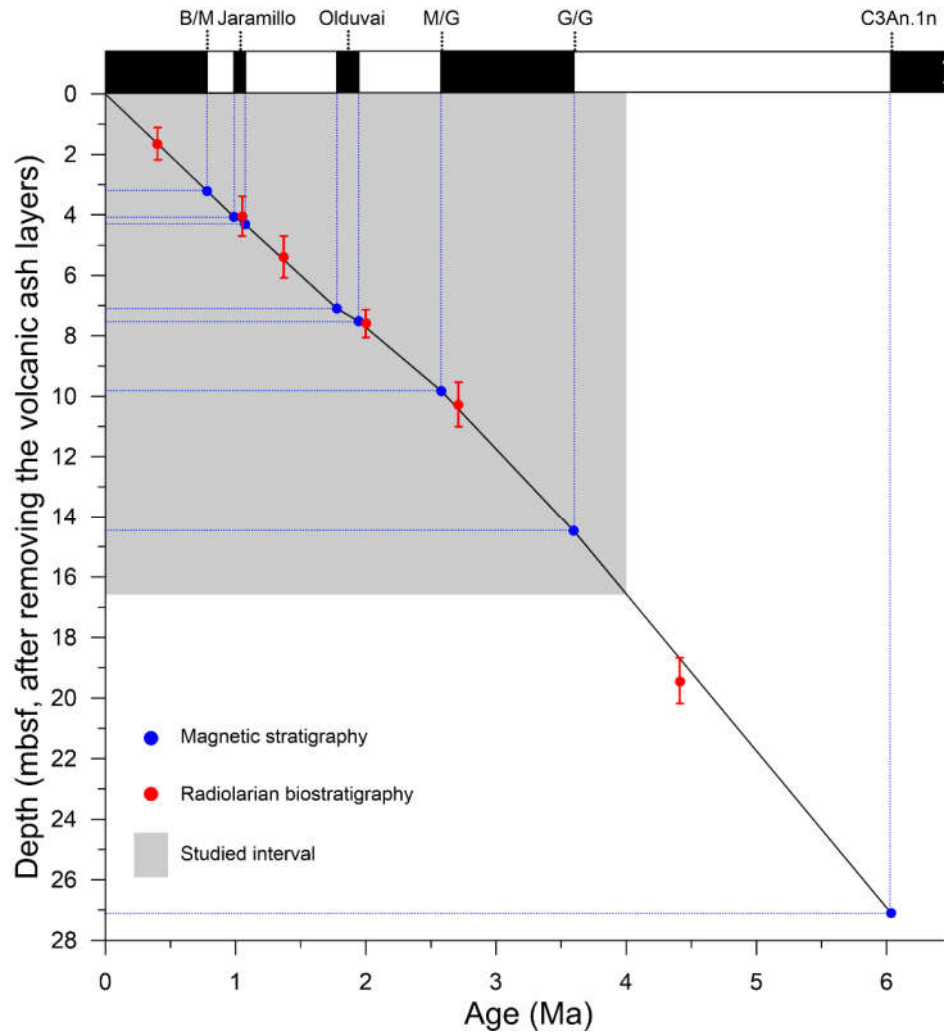**Part 1: Age-depth relationship for ODP Hole 885A**

Fig. S1. Age-depth relationship for ODP Hole 885A. Blue solid circles represent age-control points from a magnetic reversal stratigraphy for this hole (Dickens et al., 1995) based on the geomagnetic polarity time scale (GPTS) of Gradstein et al. (2012). Red solid circles with error bars represent age-control points from a radiolarian biostratigraphy for Hole 885A (Morley and Nigrini, 1995). Gray shading indicates the interval studied here (since ~ 4.0 Ma). An age model was obtained by linear interpolation from the magnetic reversal stratigraphy with age-control points of: Brunhes/Matuyama boundary = 3.21 mbsf (meters below seafloor), top Jaramillo = 4.07 mbsf, onset Jaramillo = 4.31 mbsf, top Olduvai = 7.1 mbsf, onset Olduvai = 7.52 mbsf, Matuyama/Gauss = 9.83 mbsf, Gauss/Gilbert = 14.47 mbsf, and top C3An.1n = 27.1 mbsf.

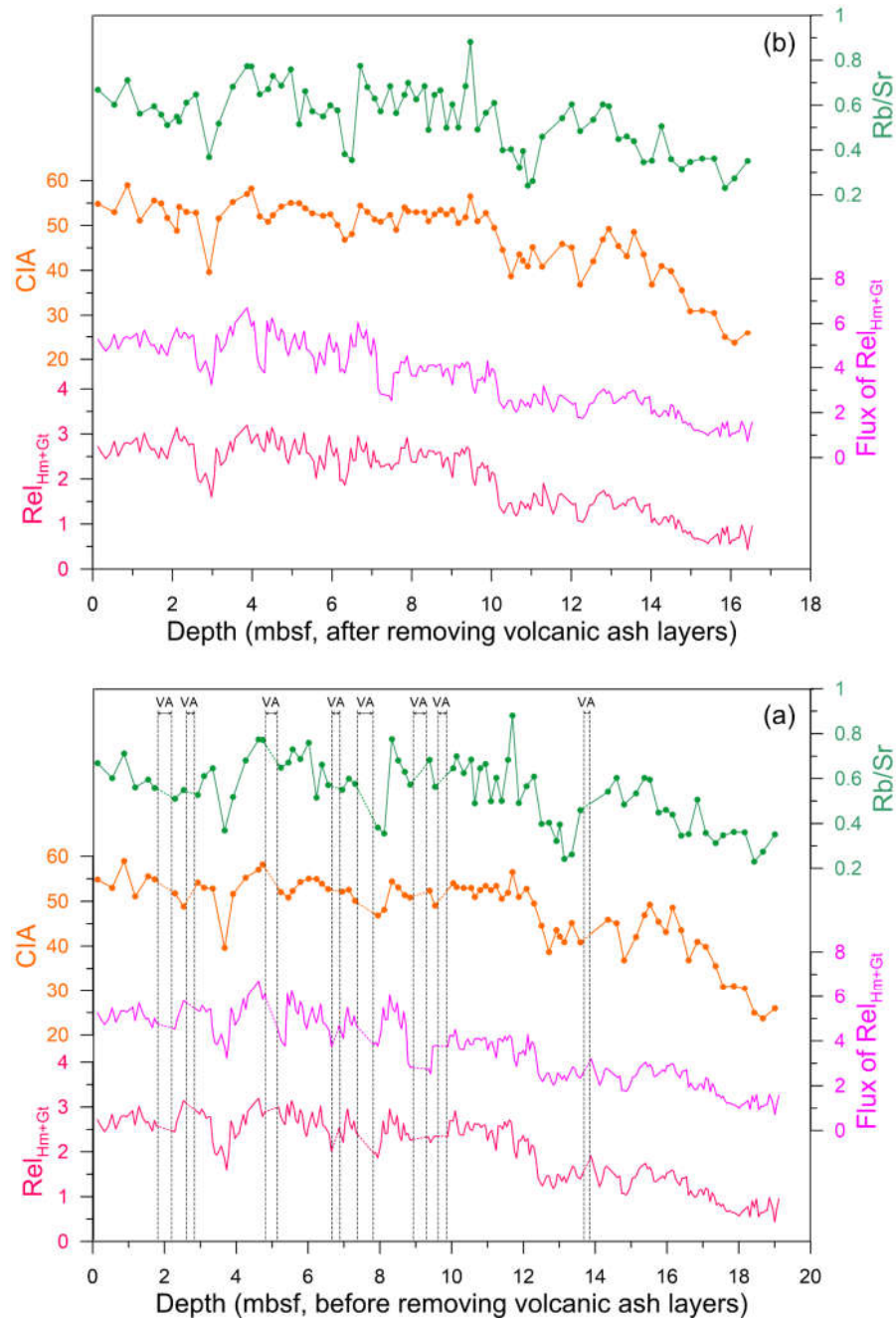**Part 2: Depth-parameter relationships before and after removal of instantaneous volcanic ash layers**

Fig. S2. Depth-parameter relationships (a) before and (b) after removing volcanic ash layers. VA: volcanic ash layers.

Part 3: Details of experimental procedures

DRS was measured for all samples using a Cary 5000 ultraviolet-visible-infrared spectrometer equipped with $BaSO_4$ as the white standard. DRS data were transformed into the

Kubelka-Munk (K-M) remission function (F(R) = (1-R)^2/2R, where R is reflectance). The corresponding band intensity for hematite and goethite from second derivative curves of F(R) and are defined as I_{Hm} and I_{Gt}, which are proportional to the concentration of hematite and goethite (Scheinost et al., 1998). Our eolian proxy is defined as: Rel_{Hm+Gt} ($Rel_{Hm+Gt_i} = n * \left(\frac{I_{Hm_i}}{\sum_{i=1}^{n} I_{Hm_i}} + \frac{I_{Gt_i}}{\sum_{i=1}^{n} I_{Gt_i}} \right)$, where n is the number of samples; Zhang et al., 2018). Rel_{Hm+Gt} represents the combined relative concentration of hematite and goethite per unit mass of dry sample. To determine the input history of a sedimentary component (Rea, 1994), we define the Rel_{Hm+Gt} flux to reflect eolian hematite and goethite inputs at Hole 885A: Flux of $Rel_{Hm+Gt} = Rel_{Hm+Gt} * DBD * LSR$ (DBD, dry bulk density; LSR, linear sedimentation rate). DBD data are calculated by linear interpolation based on Snoeckx et al. (1995).

Major and trace elements were measured for 77 approximately equispaced samples by inductively coupled plasma - optical emission spectrometry (ICP-OES, Icap-6300, ThermoFisher, USA) and inductively coupled plasma - mass spectrometry (ICP-MS, X Series II, ThermoFisher, USA), respectively. Sediments were powdered (50 mg) for elemental analysis, digested with 1.5 ml high-purity HNO_3 and 1.5 ml high-purity HF for 48 h in a tightly closed Teflon sample melting tank, and heated in an oven at < 190 °C. After cooling, samples were evaporated to incipient dryness. Dry samples were then reacted with 1.0 ml high-purity HNO_3 to remove the residual HF, and were then digested with a mixture of 3 ml 50% (volume fraction) HNO_3 and 0.5 ml rhodium (100 ppb) as an internal standard for 24 h in a tightly closed Teflon tank in an oven at 150 °C. Samples were later diluted with ultrapure water, and major and trace elements were measured by ICP-OES and ICP-MS, respectively. A national geostandard GSD-9 provided by the National Research Center for geo-analysis was injected and duplicate analyses were made for every 10 samples to provide quality control for accuracy and precision. All geochemistry measurements were made at the First Institute of Oceanography, Ministry of Natural Resources of China.

Part 4: Details of CIA calculation

CIA is given by: CIA = [Al_2O_3/(Al_2O_3+CaO^*+K_2O+Na_2O)] ×100, where CaO^* is the amount of CaO incorporated in siliceous rock. A correction should be made for carbonate and

apatite (Nesbitt and Young, 1982). ODP Hole 885A lies below the carbonate compensation depth (CCD), and carbonate has dissolved completely in this hole. ODP Hole 885A sediments contain some ichthyolith teeth, which are mainly composed of apatite (Rea et al., 1993; Ingram, 1995), so we corrected for apatite using the method of McLennan et al. (1993).
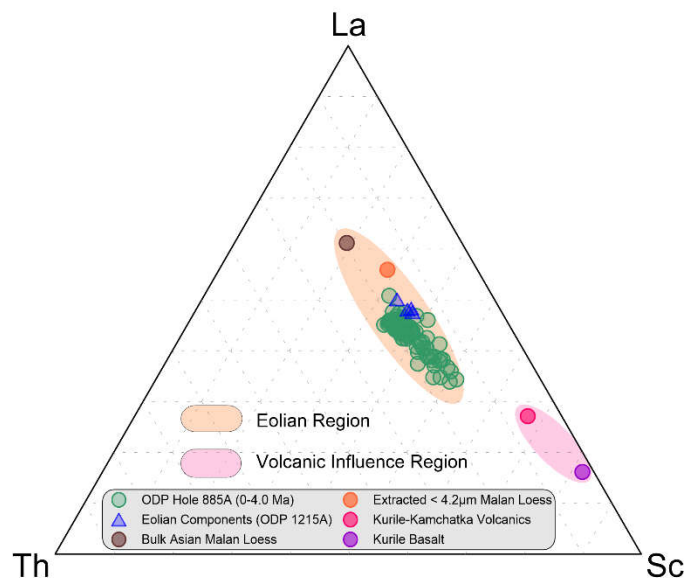
Part 5: La-Th-Sc diagram for ODP Hole 885A

Fig. S3. La–Th–Sc diagram for Asian loess data (from Weber et al. (1996)), Kurile-Kamchatka (K-K) volcanic data (from Bailey (1993)), Kurile basalt data (from Bailey et al. (1989)), and ODP Hole 1215A eolian component data (from Ziegler et al. (2007)). All data for ODP Hole 885A fall in the eolian region. Volcanic ash layers in Hole 885A (Rea et al., 1993) were excluded for sample collection and measurements; the La-Th-Sc diagram confirms that the studied-samples are not affected significantly by volcanic inputs.

Part 6: Land-ocean comparison between the Chinese Loess Plateau (CLP) and North Pacific Ocean (NPO)
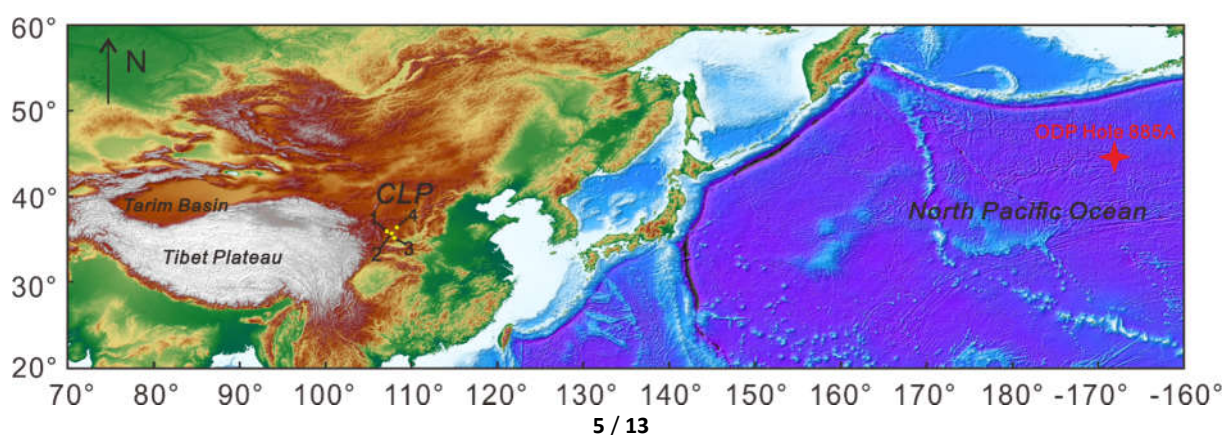
Fig. S4. Location of CLP profiles and ODP Hole 885A. The Baishui (No. 1, BS) profile is from Xiong et al. (2010), the Jingchuan (No. 2, JC) profile is from Ding et al. (2001), the Zhaojiachuan (No. 4, ZJC) and Lingtai (No. 3, LT) profiles are from Sun and An (2005).

Loess–paleosol and red clay sequences on the CLP are well-known eolian archives for documenting late Cenozoic Asian climate and environmental change (Liu, 1985; An et al., 2001; Guo et al., 2002). Land-ocean comparison between the CLP and NPO enables exploration of the paleoclimatic significance of eolian records from two major Asian dust accumulation areas (Hovan et al., 1989). For the CLP, we select the Zhaojiachuan (ZJC, 35°45′ N, 107°49′ E), Lingtai (LT, 35°04′ N, 107°39′ E), Baishui (BS, 35°24′10″ N, 106°56′43″ E), and Jingchuan (JC, 35°17′30″ N, 107°22′05″ E) profiles (Fig. S4) for the < 4.0 Ma time interval to compare with eolian and weathering records from ODP Hole 885A. Mass accumulation rates (MAR) of eolian deposits and mean grain size (MGS) of quartz in the ZJC and LT profiles are generally well correlated (Fig. S5d, S5e) (Sun and An, 2005; Sun et al., 2006). CIA was measured for the continuous Jingchuan (Sun and Zhu, 2010) and Baishui (Xiong et al., 2010) loess/paleosol-red clay sequences (Fig. S5f, S5g), respectively, and Rb/Sr was measured for the Jingchuan profile (Fig. S5h) by Sun and Zhu (2010).

Although eolian fluxes to the NPO (Fig. S5a) and CLP (Fig. S5d) are both characterized by increasing trends over the past 4.0 Ma and in response to the iNHG event, they differ in detail. CIA (Fig. S5f and S5g) and Rb/Sr (Fig. S5h) have entirely different temporal patterns for the CLP compared to ODP Hole 885A (Fig. S5b and Fig. S5c). For the pre-Quaternary period, elevated CIA values (Fig. S5f and S5g) for CLP profiles indicate that the red-clays are moderately weathered. The decreasing CIA trend reflects gradually weakened chemical weathering of loess-paleosol sequences after the iNHG event. However, Rb/Sr has nearly inverse variations compared to CIA, which indicates that it might be controlled by other factors in the CLP (Sun and Zhu, 2010).

The Gobi Desert (An, 2000; Sun, 2002; Sun et al., 2007) and the arid lands between the Qilian and Gobi-Altay Mountains (Chen and Li, 2011) are considered major dust sources for the CLP. Sun and Zhu (2010) proposed that eolian provenance for CLP changed at 2.6 Ma, and that Quaternary eolian dust tended to be derived from mainly high mountainous areas rather

than low-lying cratonic regions before 2.6 Ma. This source change could account for the Rb/Sr change (Fig. S5h) before and after the iNHG event. However, ODP Hole 885A sediments were derived mainly from Asian interior dust sources, such as Tarim Basin, over the past 12.0 Ma without significant provenance variations (Pettke et al., 2000).

For the CLP eolian record, the mean grain size of quartz (MGS, Fig. S5e) is an accepted East Asian winter monsoon (EAWM) proxy. The broadly coupled trend between MAR (Fig. S5d) and MGS (Fig. S5e), especially since the iNHG event, reflects increased eolian inputs that were controlled mainly by a stronger northwesterly surface winter monsoon in the CLP region (Sun and An, 2005; Sun et al., 2006). For the pre-Quaternary red clay, high-level westerlies has been suggested to be responsible for eolian supply (Ding et al., 1998, 2000; Vandenberghe et al., 2006; Zhang et al., 2003), while NPO eolian deposition documents a nearly continuous westerly signal since the late Cenozoic (Merrill et al, 1989; Rea, 1994). Although red clay on the CLP was deposited by westerlies, these pre-Quaternary eolian materials experienced intense post-depositional chemical weathering and pedogenesis, as indicated by higher CIA (Fig. S5f and S5g; Xiong et al., 2010; Sun and Zhu, 2010) and abundant pedogenic hematite (Hao et al., 2008, 2009; Maher, 2016). Hence, information about the westerlies has been altered in red clay sequences. In contrast, Asian eolian fractions transported by westerlies are well preserved in the stable NPO deep-sea environment without significant post-depositional alteration (Rea, 1994).

From the above interpretation, provenance, transportation, and post-depositional alteration of CLP sediments are controlled by both Asian winter and summer monsoons, while the NPO deep-sea eolian archive documents an original westerly signal from Asian inland dust source areas. Therefore, eolian records and corresponding weathering indices have their own distinct patterns. The post-iNHG moisture increase mechanism in Asian dust source regions proposed here is based mainly on the strong positive relationship between eolian flux and weathering proxies. Other mechanisms might account for variation of these records and proxies. Further eolian dust studies, such as development of long-term marine eolian records from Asian marginal seas and the Northwest and North Pacific Ocean, and recovery of high-resolution terrestrial westerly-deposited signals, will enable the detailed land-ocean comparisons needed to assess the proposed mechanism for the post-iNHG moisture increase and to assess other

potential explanations. Nevertheless, this study provides a new perspective for understanding the paleoclimatic significance of NPO eolian records.
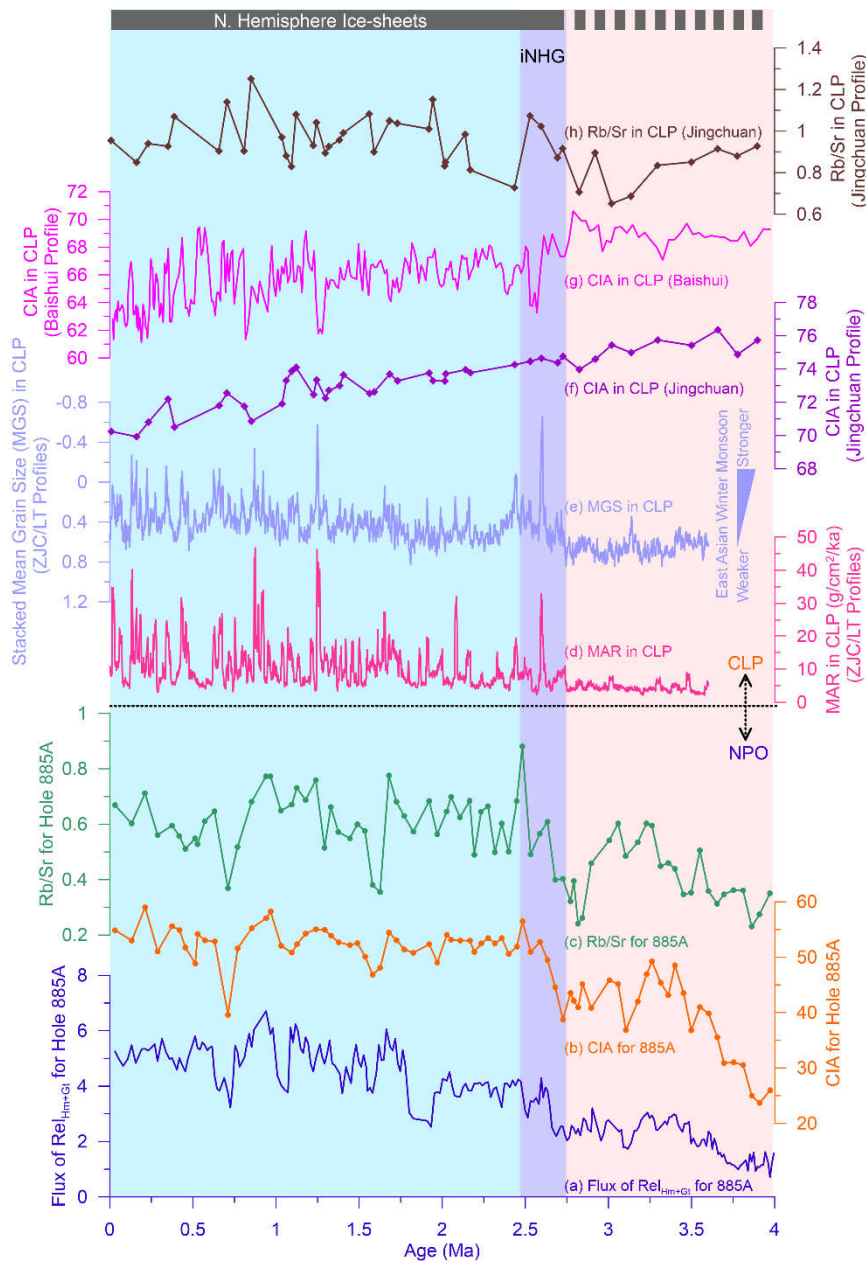

Fig. S5. Land-ocean comparison between the Chinese Loess Plateau (CLP) and North Pacific Ocean (NPO). a, Flux of Rel$_{Hm+Gt}$ for ODP Hole 885A; b, CIA for ODP Hole 885A; c, Rb/Sr for ODP Hole 885A; d, mass accumulation rates (MAR) for the CLP Zhaojiachuan/Lingtai profiles (Sun and An, 2005); e, stacked mean grain size of quartz for the CLP Zhaojiachuan/Lingtai profiles (Sun et al., 2006); f, CIA for the CLP Jingchuan profile (Sun and Zhu, 2010); g, CIA for the CLP Baishui profile (Xiong et al., 2010); h, Rb/Sr for the CLP Jingchuan profile (Sun and Zhu, 2010). Black bars at the top of the figure indicate the development process of northern hemisphere ice-sheets (Zachos et al., 2001).

References

An, Z., 2000, The history and variability of the East Asian paleomonsoon climate: Quaternary Science Reviews, v. 19(1–5), p. 171–187, doi: 10.1016/s0277-3791(99)00060-8.

An, Z. S., Kutzbach, J. E., Prell, W. L., and Porter, S. C., 2001, Evolution of Asian monsoons and phased uplift of the Himalaya-Tibetan plateau since late Miocene times: Nature, v. 411, p. 62–66, doi: 10.1038/35075035.

Bailey, J. C., 1993, Geochemical history of sediments in the northwestern Pacific Ocean: Geochemical Journal, v. 27(2), p. 71–90, doi: 10.2343/geochemj.27.71.

Bailey, J. C., Frolova, T. I., and Burikova, I. A., 1989, Mineralogy, geochemistry and petrogenesis of Kurile island-arc basalts: Contributions to Mineralogy and Petrology, v. 102(3), p. 265–280, doi: 10.1007/BF00373720.

Chen, J., and Li, G., 2011, Geochemical studies on the source region of Asian dust: Science China Earth Sciences, v. 54(9), p. 1279–1301, doi: 10.1007/s11430-011-4269-z.

Dickens, G. R., Snoeckx, H., Arnold, E., Morley, J. J., Owen, R. M., Rea, D. K., and Ingram, L., 1995, Composite depth scale and stratigraphy for Sites 885/886: Proceedings of the Ocean Drilling Program, Scientific Results, v. 145, p. 205–217.

Ding, Z. L., Sun, J. M., Liu, T. S., Zhu, R. X., Yang, S. L., and Guo, B., 1998, Wind-blown origin of the Pliocene red clay formation in the central Loess Plateau, China: Earth and Planetary Science Letters, v. 161(1–4), p. 135–143, doi: 10.1016/s0012-821x(98)00145-9.

Ding, Z. L., Yang, S. L., Hou, S. S., Wang, X., Chen, Z., and Liu, T. S., 2001, Magnetostratigraphy and sedimentology of the Jingchuan red clay section and correlation of the Tertiary eolian red clay sediments of the Chinese Loess Plateau: Journal of Geophysical Research: Solid Earth, v. 106(B4), p. 6399–6407, doi: 10.1029/2000jb900445.

Ding, Z. L., Rutter, N. W., Sun, J. M., Yang, S. L., and Liu, T. S., 2000, Re-arrangement of atmospheric circulation at about 2.6 Ma over northern China: evidence from grain size records of loess-palaeosol and red clay sequences: Quaternary Science Reviews, v. 19(6), p. 547–558, doi: 10.1016/S0277-3791(99)00017-7.

Guo, Z. T., Ruddiman, W. F., Hao, Q. Z., Wu, H. B., Qiao, Y. S., Zhu, R. X., Peng, S. Z., Wei, J. J., Yuan, B. Y., and Liu, T. S., 2002, Onset of Asian desertification by 22 Myr ago inferred from loess deposits in China: Nature, v. 416, p. 159–163, doi: 10.1038/416159a.

Gradstein, F. M., Ogg, J. G., Schmitz, M., and Ogg, G., 2012, The geologic time scale 2012. Elsevier, doi: 10.1016/B978-0-444-59425-9.18001-1.

Hao, Q., Oldfield, F., Bloemendal, J., and Guo, Z., 2008, The magnetic properties of loess and paleosol samples from the Chinese Loess Plateau spanning the last 22 million years: Palaeogeography, Palaeoclimatology, Palaeoecology, v. 260(3–4), p. 389–404, doi: 10.1016/j.palaeo.2007.11.010.

Hao, Q., Oldfield, F., Bloemendal, J., Torrent, J., and Guo, Z., 2009, The record of changing hematite and goethite accumulation over the past 22 Myr on the Chinese Loess Plateau from magnetic measurements and diffuse reflectance spectroscopy: Journal of Geophysical Research: Solid Earth, v. 114(B12), doi: 10.1029/2009JB006604.

Hovan, S. A., Rea, D. K., Pisias, N. G., and Shackleton, N. J., 1989, A direct link between the China loess and marine $\delta^{18}O$ records: aeolian flux to the North Pacific: Nature, v. 340(6231), p. 296–298, doi: 10.1038/340296a0.

Ingram, B. L., 1995, Ichthyolith strontium isotopic stratigraphy of deep-sea clays: Sites 885 and 886 (North Pacific transect). In Proceedings of the Ocean Drilling Program, Scientific Results, v. 145, p. 399–412.

Liu, T., 1985, Loess and the Environment. China Ocean Press, Beijing.

Maher, B. A., 2016, Palaeoclimatic records of the loess/palaeosol sequences of the Chinese Loess Plateau: Quaternary Science Reviews, v. 154, p. 23–84, doi: 10.1016/j.quascirev.2016.08.004.

McLennan, S. M., Hemming, S., McDaniel, D. K., and Hanson, G. N., 1993, Geochemical approaches to sedimentation, provenance, and tectonics: Special Papers-Geological Society of America, v. 284, p. 21–40, doi: 10.1130/SPE284-p21.

Merrill, J. T., Uematsu, M., and Bleck, R., 1989, Meteorological analysis of long range transport of mineral aerosols over the North Pacific: Journal of Geophysical Research: Atmospheres, v. 94(D6), p. 8584–8598, doi: 10.1029/JD094iD06p08584.

Morley, J. J., and Nigrini, C., 1995, Miocene to Pleistocene radiolarian biostratigraphy of North Pacific Sites 881, 884, 885, 886, and 887, In Proceedings of the Ocean Drilling Program, Scientific Results, v. 145, p. 55–91.

Nesbitt, H. W., and Young, G. M., 1982, Early Proterozoic climates and plate motions inferred from major element chemistry of lutites: Nature, v. 299(5885), p. 715–717, doi: 10.1038/299715a0.

Pettke, T., Halliday, A. N., Hall, C. M., and Rea, D. K., 2000, Dust production and deposition in Asia and the north Pacific Ocean over the past 12 Myr: Earth and Planetary Science Letters v. 178(3), p. 397–413, doi: 10.1016/S0012-821X(00)00083-2.

Rea, D. K., 1994, The paleoclimatic record provided by eolian deposition in the deep sea. The geologic history of wind: Reviews of Geophysics, v. 32(2), p. 159–195, doi: 10.1029/93RG03257.

Rea, D. K., Basov, I. A., Janecek, T. R., Palmer-Julson, A., et al., 1993, Sites 885/886: In Proceedings of the Ocean Drilling Program, Initial Reports, v. 145, p. 303–334.

Scheinost, A. C., Chavernas, A., Barrón, V., and Torrent, J., 1998, Use and limitations of second-derivative diffuse reflectance spectroscopy in the visible to near-infrared range to identify and quantity Fe oxide minerals in soils: Clays and Clay Minerals, v. 46(5), p. 528–536, doi.org/10.1346/CCMN.1998.0460506.

Snoeckx, H., Rea, D. K., Jones, C. E., and Ingram, B. L., 1995, Eolian and silica deposition in the central North Pacific: results from sites 885/886: Proceedings of the Ocean Drilling Program, Scientific Results, v. 145, p. 219–230.

Sun, J., 2002, Provenance of loess material and formation of loess deposits on the Chinese Loess Plateau: Earth and Planetary Science Letters, v. 203(3–4), p. 845–859.

Sun, J., and Zhu, X., 2010, Temporal variations in Pb isotopes and trace element concentrations within Chinese eolian deposits during the past 8 Ma: implications for provenance change: Earth and Planetary Science Letters, v. 290(3–4), p. 438–447, doi: 10.1016/j.epsl.2010.01.001.

Sun, Y., and An, Z., 2005, Late Pliocene‐Pleistocene changes in mass accumulation rates of eolian deposits on the central Chinese Loess Plateau: Journal of Geophysical Research: Atmospheres, v. 110(D23), doi: 10.1029/2005JD006064.

Sun, Y., Clemens, S. C., An, Z., and Yu, Z., 2006, Astronomical timescale and palaeoclimatic implication of stacked 3.6-Myr monsoon records from the Chinese Loess Plateau: Quaternary Science Reviews, v. 25(1–2), p. 33–48, doi:10.1016/j.quascirev.2005.07.005.

Sun, Y., Tada, R., Chen, J., Chen, H., Toyoda, S., Tani, A., ... and Ji, J., 2007, Distinguishing the sources of Asian dust based on electron spin resonance signal intensity and crystallinity of quartz: Atmospheric Environment, v. 41(38), p. 8537–8548, doi: 10.1016/j.atmosenv.2007.07.014.

Vandenberghe, J., Renssen, H., van Huissteden, K., Nugteren, G., Konert, M., Lu, H., ... and Buylaert, J. P., 2006, Penetration of Atlantic westerly winds into Central and East Asia: Quaternary Science Reviews, v. 25(17–18), p. 2380–2389, doi: 10.1016/j.quascirev.2006.02.017.

Weber, E. T., Owen, R. M., Kent-Corson, G. R., Halliday, A. N., Jones, C. E., and Rea, D. K., 1996, Quantitative resolution of eolian continental crustal material and volcanic detritus in North Pacific surface sediment: Paleoceanography, v. 11(1), p. 115–127, doi: 10.1029/95PA02720.

Xiong, S., Ding, Z., Zhu, Y., Zhou, R., and Lu, H., 2010, A ~6 Ma chemical weathering history, the grain size dependence of chemical weathering intensity, and its implications for provenance change of the Chinese loess–red clay deposit: Quaternary Science Reviews, v. 29(15–16), p. 1911–1922, doi:10.1016/j.quascirev.2010.04.009.

Zachos, J., Pagani, M., Sloan, L., Thomas, E., and Billups, K., 2001, Trends, rhythms, and aberrations in global climate 65 Ma to present: Science, v. 292(5517), p. 686–693, doi: 10.1126/science.1059412.

Zhang, Q., Liu, Q., Li, J., and Sun, Y., 2018, An integrated study of the eolian dust in pelagic sediments from the North Pacific Ocean based on environmental magnetism, transmission electron microscopy, and diffuse reflectance spectroscopy: Journal of Geophysical Research: Solid Earth, v. 123, p. 3358–3376, doi: 10.1002/2017JB014951.

Zhang, X. Y., Gong, S. L., Zhao, T. L., Arimoto, R., Wang, Y. Q., and Zhou, Z. J., 2003, Sources of Asian dust and role of climate change versus desertification in Asian dust emission: Geophysical Research Letters, v. 30(24), doi: 10.1029/2003gl018206.

Ziegler, C. L., Murray, R. W., Hovan, S. A., and Rea, D. K., 2007, Resolving eolian, volcanogenic, and authigenic components in pelagic sediment from the Pacific Ocean: Earth and Planetary Science Letters, v. 254(3), p. 416–432, doi: 10.1016/j.epsl.2006.11.049.